Subharmonic instabilities of Tollmien-Schlichting waves in two-dimensional Poiseuille flow

A. Drissi, M. Net, and I. Mercader
Universitat Politècnica de Catalunya, Jordi Girona Salgado s/n. Campus Nord. Mòdul B-4, 08034 Barcelona, Spain
(Received 14 August 1998; revised manuscript received 17 May 1999)

The stability of the *upper branch* of shear traveling waves in two-dimensional Poiseuille flow, when the total flux through the channel is held constant, is considered. Taking into account the length of the periodic channel, perturbations of the same wave number (superharmonic), and different wave number (subharmonic) of the uniform wave trains are imposed. We mainly consider channels long enough to contain $M=4$ and $M=8$ basic wavelengths. In these cases, subharmonic bifurcations are found to be dominant except in a small region of parameters. From this type of bifurcation, we show that if the wave number is decreased, the periodic train of finite amplitude waves evolves continuously towards the stable localized wave packets obtained in long channels by other authors and whose existence has been associated to the vicinity of an inverted Hopf bifurcation. Depending on the basic wave number of the periodic train destabilized, different types of solutions for a given length of the channel can be obtained. Furthermore, for moderate Reynolds numbers, configurations of linearly stable wave trains exist, provided that their basic wave number is $\alpha \approx 1.5$. [S1063-651X(99)15208-5]

PACS number(s): 47.20.Ft, 47.20.Lz, 47.20.Ky

I. INTRODUCTION

Although it is known that the transition to turbulence in wall-bounded flows is three-dimensional (3D), several authors [1–3] have shown interest in the study of pure 2D flows in spatially periodic Poiseuille flow, because many properties of the 2D flows obtained are observed in fully turbulent three-dimensional flows. This system is a good model to look for two-dimensional turbulence, since unlike other 2D flows, the basic flow becomes linearly unstable and develops finite-amplitude two-dimensional waves [4], which in turn become unstable and lead to more complicated motions. In [5], the author established the hypothesis that the transition from the laminar state to the turbulent state is dependent on the existence of intermediate vortical states, and that the transition to turbulence is the three-dimensional instability of these states. These vortical states could be either two-dimensional traveling waves, quasiperiodic solutions, or three-dimensional waves. The more information about the existence of 2D attractors we can obtain, the better three-dimensional transitions can be established. Bearing this in mind, our goal is to supply more information about the 2D scenario, analyzing the successive bifurcations that may lead to different 2D flows obtained for moderated Reynolds numbers.

In plane Poiseuille flow, neither the critical Reynolds number for the instability of the basic flow nor the critical Reynolds number for the existence of the two-dimensional waves coincides with the experimentally observed critical Reynolds number when finite-amplitude disturbances are considered. Then, the two-dimensional wave trains which bifurcate subcritically from the basic flow are only the first step of the transition. The stability of the uniform wave trains have been studied by two different approaches. One is performed by time-dependent numerical simulations of the disturbances (see Refs. [1,2,6,7] among others). The other, based on the fact that traveling waves are steady solutions in a moving frame of reference, uses the customary stability analysis (see Refs. [8,3] for the 2D case and [9] for the 3D case). Using this last approach [8], and [3] considered superharmonic disturbances of a uniform wave train of wave number $\alpha=1.1$. The values of the Reynolds number and period of the Hopf bifurcation they obtained agree quite well with the results of [1] and [2] for short periodic boxes, employing the first approach. If the box is long enough to contain several wavelengths, the results of [2] and [7] (for basic wavelength $a=2\pi$) reveal the existence of stable and attracting localized wave packets that appear for moderate values of the Reynolds number. These authors link the presence of these solutions with the vicinity of a subcritical Hopf bifurcation. The connection is justified by the works of [10] and [11], in which structurally stable pulse solutions of the corresponding complex Ginsburg-Landau equation including a quintic nonlinearity were obtained. However, [10] showed that the necessary condition for the existence of this type of solution is more restrictive than the condition for the existence of a subcritical Hopf bifurcation. In addition, [2] pointed out the possibility of obtaining different configurations depending on the initial conditions used in his time-dependent simulations.

This paper is devoted to analyzing the two-dimensional stability of the 2D uniform wave trains in plane Poiseuille flow to both superharmonic and subharmonic bifurcations when a constant flux is imposed as a longitudinal boundary condition. By using the second approach quoted above, we analyze superharmonic bifurcations, extending the calculations of [3] for any value of α. With a technique similar to [12] used in Rayleigh-Bénard convection, we analyze subharmonic bifurcations in boxes that contain $M=4$ and $M=8$ basic wavelengths of any basic periodicity. We also present a series of nonperiodic solutions obtained from time-dependent numerical simulations to show that the wave packets obtained by [2] and [7] come from a subharmonic bifurcation of the uniform wave trains. This instability is also responsible for the coexistence of different configurations for the same periodic channel. Another important point we wish to emphasize is that, according to our stability analysis, a stable structure of uniform wave trains can exist, even in

long boxes, for some values of the parameters: Reynolds number and basic wave number.

The paper is organized as follows. In Sec. II we derive the equations and boundary conditions, explaining the two ordinary parametrizations used in this problem, to make references to the results of other authors more understandable. In this section we also present the method used to analyze both superharmonic and subharmonic instabilities and nonperiodic solutions. The results are given in Sec. III and the paper concludes with a discussion in Sec. IV.

II. EQUATIONS AND NUMERICAL METHOD

Plane Poiseuille flow is established between two horizontal plates and is driven by a streamwise pressure gradient. We have chosen horizontal plates placed at $y=\pm h$ and the x coordinate in the direction of this gradient.

The two-dimensional, incompressible, and viscous flow will be governed by the Navier-Stokes equations

$$\frac{\partial \mathbf{u}}{\partial t}+(\mathbf{u}\cdot\nabla)\mathbf{u}=-\nabla\pi+\nu\nabla^2\mathbf{u}, \tag{2.1a}$$

$$\nabla\cdot\mathbf{u}=0, \tag{2.1b}$$

where $\mathbf{u}=(u,v)$ and π is the pressure field over density. No-slip boundary conditions at the horizontal plates implies $\mathbf{u}(x,\pm h,t)=0$. If the pressure gradient has a uniform x average P', these equations and boundary conditions admit an exact solution with a parabolic velocity profile $\mathbf{u}_b=U_0(1-y^2/h^2,0)$, known as the basic laminar solution, and where U_0 is related to P' in the following way: $U_0=-h^2P'/2\nu$. For this solution the flux through the channel is $Q'=4hU_0/3$.

We introduce a stream function $\Psi'(x,y,t)$, related to the two components of the velocity field by $u=\Psi'_y$, $v=-\Psi'_x$, and we expand Ψ' in the following way

$$\Psi'(x,y,t)=U_0\left(y-\frac{y^3}{3h^2}\right)+\sum_{-N}^{N}\Psi'_n(y,t)e^{in\alpha x},$$

with the value of U_0 unspecified and being α the wave number associated with the length L of the periodic channel. The reality of Ψ' implies

$$\Psi'_{-n}(y,t)=\tilde{\Psi}'_n(y,t),$$

where the tilde denotes complex conjugate. Scaling lengths by the channel half width h, velocities by U_0, and eliminating the prime to denote dimensionless quantities, Eqs. (2.1a) and (2.1b) are equivalent to the stream function formulation

$$\frac{\partial\nabla^2\Psi}{\partial t}+\Psi_y\nabla^2\Psi_x-\Psi_x\nabla^2\Psi_y=\frac{1}{\mathrm{Re}}\nabla^4\Psi, \tag{2.2}$$

where Re is the Reynolds number

$$\mathrm{Re}=\frac{hU_0}{\nu}.$$

The modal no-slip boundary conditions are

$$\frac{\partial\Psi_n}{\partial y}=0 \text{ at } y=\pm h, n\geq 0, \tag{2.3a}$$

$$\Psi_n=0 \text{ at } y=\pm h,\ n>0. \tag{2.3b}$$

Since we will solve Eq. (2.2) for every Fourier mode, we still need to specify two additional boundary conditions for Ψ_0. As Ψ is arbitrary to within a constant, we set $\Psi_0(-1)=0$ and one boundary condition is still undetermined. This fact is associated with not having yet chosen the value of U_0.

Our choice is to fix the average flux Q', and set $U_{0,Q}=3Q'/4h$. Then, the other boundary condition for Ψ_0 will be $\Psi_0(+1)=0$. The Reynolds number is related with the average flux Q' by $\mathrm{Re}_Q=3Q'/4\nu$, the dimensionless flux Q will always be $Q=\frac{4}{3}$, and the dimensionless uniform average pressure gradient P_Q for this parametrization of the problem is

$$P_Q(t)=-\frac{2}{\mathrm{Re}_Q}\left(1-\frac{1}{4}[\Psi^Q_{0,yy}(1,t)-\Psi^Q_{0,yy}(-1,t)]\right), \tag{2.4}$$

where index Q means that all quantities refer to a constant flux parametrization.

Other authors have used as a different parametrization of the problem the fixing of a constant average pressure gradient P', and setting the value $U_{0,p}$ as $U_{0,p}=-h^2P'/2\nu$. Then, the Reynolds number is related to P' as $\mathrm{Re}_p=-h^3P'/2\nu^2$, the dimensionless average pressure gradient is $P=-2/\mathrm{Re}_p$, and the dimensionless flux Q_p is

$$Q_p(t)=\frac{4}{3}+[\Psi^p_0(1,t)-\Psi^p_0(-1,t)], \tag{2.5}$$

where the index p means that all quantities refer to a constant average pressure gradient parametrization.

This parametrization is the usual one when a formulation in primitive variables $(\mathbf{u},p)$ is used [6,13], or in other formulations whenever the x-momentum equation for the zero Fourier mode of the x component of the velocity (as independent variable) is a governing equation [9]. However, if a stream function formulation for the 2D case is used with this parametrization, as discussed in detail in [3], the additional boundary condition for the dimensionless stream function Ψ^p_0 is obtained from the x average of the Navier-Stokes equation in the x direction and integrating over the channel width. This boundary condition is

$$\frac{\partial\Psi^p_0}{\partial t}(+1,t)-\frac{\partial\Psi^p_0}{\partial t}(-1,t)=-\frac{1}{\mathrm{Re}_p}[\Psi^p_{0,yy}(1,t)-\Psi^p_{0,yy}(-1,t)]. \tag{2.6}$$

Notice that the left hand side of this equation coincides with $\partial Q_p(t)/\partial t$.

For the basic laminar flow $\mathrm{Re}_p=\mathrm{Re}_Q$, and its stability to infinitesimal 2D disturbances of the form $\Phi(y,x,t)=\Phi(y)e^{i\alpha x}e^{\lambda t}$ gives rise to the marginal stability curve $\Re[\lambda(\mathrm{Re},\alpha)]=0$, obtained by minimizing the Reynolds number for every α (Here $\Re$ indicates the real part). This curve, labeled R_b, is represented in Fig. 1. This bifurcation

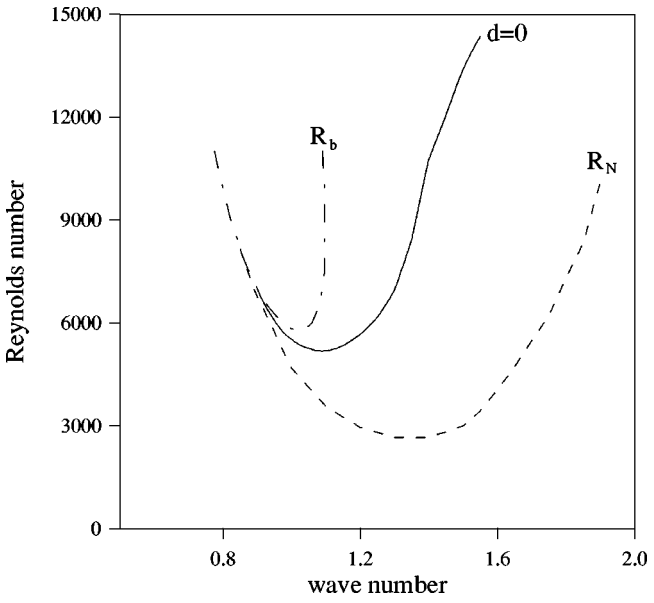

FIG. 1. Critical Reynolds number versus the wave number α for different types of bifurcations. The dash-dotted line (labeled R_b) corresponds to the bifurcation of the parabolic profile, the dashed line (labeled R_N) corresponds to the minimum Reynolds number for which periodic traveling waves appear, and the solid line (labeled $d=0$) corresponds to superharmonic bifurcations of the waves belonging to the *upper branch*.

is in general subcritical, and the new solution consists in a family of periodic traveling shear waves. If one defines a characteristic amplitude of these waves—the disturbance energy, for example—and fixes α varying the Reynolds number near the bifurcation point, the *lower branch* for decreasing Reynolds number is obtained. When it reaches a value $R_N(\alpha)$, the amplitude turns around towards higher Reynolds numbers, increasing its value and forming the *upper branch*. As is known [14], the *lower branch* is unstable to 2D superharmonic bifurcations. For these steady wave trains, the Reynolds numbers corresponding to two different parametrizations of the problem are related by the expression

$$\mathrm{Re}_p = \mathrm{Re}_Q\left(1-\frac{1}{4}[\Psi^Q_{0,yy}(1)-\Psi^Q_{0,yy}(-1)]\right), \qquad (2.7)$$

and represent only different scaling of the problem [3]. In this case, since Ψ^Q_0 and Ψ^p_0 are time independent, if one fixes the average flux Q, P_Q is time independent, and so is Q_p if one fixes the average pressure gradient [see Eqs. (2.4) and (2.5)]. For this last parametrization, since Q_p is time independent, $\Psi^p_{0,yy}(1)=\Psi^p_{0,yy}(-1)$.

There exist other two-dimensional solutions, described in [13] and obtained for wave numbers $\alpha\approx 0.3$, (*long-wavelength secondary flows*), for which Q_p and P_Q are both time independent, but are not traveling waves. This fact can only be explained if

$$\Psi^p_{0,yy}(1,t)=\Psi^p_{0,yy}(-1,t)$$

is satisfied. For these solutions this value is zero, which can be deduced from Figs. 6 and 7 of that paper.

As far as the numerical method is concerned, we compute the steady traveling waves by assuming time independent coefficients a_{nj} in the expansion of $\Psi(x,y,t)$:

$$\Psi_{TW}(x,y,t)=\Psi_b+\sum_{n=-N}^{N}\sum_{j=0}^{J} a_{nj}g_j(y)e^{in\alpha(x-ct)}, \qquad (2.8)$$

where $g_j(y)$ is a function satisfying the boundary conditions, composed of a superposition of Tchebyshev polynomials. $g_j(y)$ is symmetric for j even and antisymmetric for j odd. Letting $\tilde{x}=x-ct$, we solve the steady equation

$$(\Psi_y-c)\nabla^2\Psi_{\tilde{x}}-\Psi_{\tilde{x}}\nabla^2\Psi_y-\frac{1}{\mathrm{Re}_Q}\nabla^4\Psi=0,$$

obtained from Eq. (2.2), by a Galerkin technique in $\tilde{x}$ and a collocation method in y. For given values of Re and α, the algebraic equations for the coefficients a_{nj} are solved by a Newton-Raphson iteration method. Since the phase of the traveling waves is arbitrary, we fix it by prescribing

$$\int_{-1}\sum_{j=0}^{J}\Im(a_{1j})g_j(y)=0,$$

where $\Im(a_{1,j})$ denotes the imaginary part of $a_{1,j}$. The corresponding equation serves for the determination of the phase velocity c. To obtain these type of solutions a truncation $N=4$ and $J=40$ is performed in the developments. Considering $N>4$ and $J>40$ causes no significant changes in the disturbance energy and phase velocity of a given solution.

To study the stability of the two-dimensional waves we proceed in the same way as [12]. We are interested in analyzing the case where the periodic box is long enough to contain M basic wavelengths a, $\alpha=2\pi/a$ being the basic wave number. Since the waves are steady in a moving frame of reference, we can apply the usual stability analysis.

The basic solution has period a, and hence the associated linear operator also has period a. We use Floquet theory to split the set of perturbations to be considered as

$$\{\Psi^*_m(\tilde{x},y,t)=\Psi_m(\tilde{x},y)e^{id_m\alpha\tilde{x}}e^{\lambda_m t}\}_{m=0,\ldots,M-1}, \qquad (2.9a)$$

where

$$\Psi_m(\tilde{x},y)=\Psi_m(\tilde{x}+a,y) \qquad (2.9b)$$

and $d_m=m/M$. Thus $\Psi^*_m(\tilde{x},y,t)$ admits the following development

$$\Psi^*_m(\tilde{x},y,t)=\sum_{n=-N}^{N}\sum_{j=0}^{J} b_{nj}g_j(y)e^{i(n+d_m)\alpha\tilde{x}}e^{\lambda_m t}. \qquad (2.10)$$

The case $d=0$ corresponds to superharmonic disturbances, and has been considered by [3] for $\alpha=1.1$. In this case, the perturbation has the same wavelength as the two-dimensional waves, and the solution that bifurcates still con-

tains M basic wavelengths. In this stability analysis, we always obtain a zero eigenvalue corresponding to the trivial phase shift solution [8].

In the case $d \neq 0$, subharmonic disturbances are considered, the basic periodicity a is now broken, and a new solution with a larger basic period emerges. As discussed in [12], the eigenfunctions for the problem with d_{M-m} can be obtained by conjugating those with d_m; in addition, $\lambda_{M-m} = \tilde{\lambda}_m$. Then it suffices to consider perturbations with $d_m \in (0,1/2]$. If a bifurcation of a shear traveling wave with phase velocity c of this type exists [$\Re(\lambda)=0$], new subharmonic wave numbers $\alpha_n=(n+d_m)\alpha$ and $\alpha'_n=(n+d_{M-m})\alpha$ appear. The corresponding frequencies are, respectively, $\omega_n=(n+d_m)\alpha c+\omega^*$ and $\omega'_n=(n+d_{M-m})\alpha c-\omega^*$, where $\omega^*=-\Im(\lambda_m)$. Then, for the bifurcated solution near a pair of frequencies and wave numbers $(\omega_{0n}=n\alpha c, \alpha_{0n}=n\alpha)$ of the basic solution, two pairs (ω_n,α_n) and $(\omega'_{n-1},\alpha'_{n-1})$ appear, which allows us to estimate a group velocity as

$$c_g \approx c+\frac{\omega^*}{d_m\alpha}. \tag{2.11}$$

Notice that the linear subharmonic stability analysis corresponding to a value d_m for a box that contains M basic wavelengths coincides with that corresponding to a value $d_{m/k}$ for a box that contains M/k ones, provided that m/k and M/k are integer. We call the *equivalent* subharmonic analysis d_{m*}, M^*, that which corresponds to the minimum pairs of integers values m/k and M/k. For example, a subharmonic stability d_3 for a box that contains $M=6$ basic wavelengths has the *equivalent* subharmonic analysis $d_{m*}=d_1$, $M^*=2$.

To obtain quantitative convergence in the superharmonic and subharmonic stability, it is necessary to use a less severe truncation than that allowed in the case of obtaining traveling waves. This subject will be discussed in detail in subsequent sections.

The integration in time of the problem (2.2) with the corresponding boundary conditions in the case of fixing the average flux is carried out by using a semimplicit second order stiffly stable scheme, Fourier-Galerkin in x and Chebyshev collocation in the y direction . Because this part of the work is devoted to showing how subharmonic instabilities act on Tollmien-Schlichting waves, the number of Fourier modes used varies depending on the number M that are extended periodically. The Fourier nonlinear term is calculated pseudospectrally, increasing the number of modes ($\frac{3}{2}N$) to obtain a de-aliased evaluation. A minimum of 64 Chebyshev modes is used in vertical direction.

III. RESULTS

In two parts of this section we present results corresponding to superharmonic and subharmonic bifurcations. Traveling wave solutions then need to be computed to analyze their stability. As a test of our code, we have reproduced the values $R_{N,p}$, scaling our value $R_{N,Q}$ by using Eq. (2.7), and phase speeds at these points, for different wave numbers α, obtained by [15] and [3].

As discussed in [15], the more unstable mode at the bifurcation of the basic flow is known to be symmetric in y; then in the expansion (2.8) of the bifurcating traveling waves in the *lower branch*, all coefficients a_{nj} with $n+j$ even vanish. So the nonlinear mean flow

$$U(y)=(1-y^2)+\sum_{j=0}^{J} a_{0j}\frac{\partial g_j(y)}{\partial y} \tag{3.1}$$

is a symmetric function of y ($a_{0j}=0$, if $j=\dot{2}$). Thus, for this type of solution, Ψ_{TW} has the following symmetry:

$$\Psi(x,y,t)=-\Psi\left(x+\frac{a}{2},-y,t\right). \tag{3.2}$$

Traveling wave solutions belonging to the *upper branch* also have this symmetry, and a symmetry breaking, if present, can be detected with our stability analysis. Because of this symmetry, disturbances of the form (2.10) separate into two classes: *odd* disturbances with vanishing coefficients b_{nj} for even $n+j$ and *even* disturbances with vanishing coefficients b_{nj} for odd $n+j$. This analysis looks very similar to the case of symmetric thermal Rossby waves in the small-gap approximation studied by [16], since these waves have the same symmetry as the traveling waves we analyze.

A. Superharmonic bifurcations

In this section we present the results corresponding to superharmonic bifurcations. This analysis has two meanings; first, it is the complete stability analysis corresponding to a periodic box whose length L coincides with $2\pi/\alpha$ ($M=1$); second, for a periodic box that contains M basic wavelengths, this is the case in which perturbations of the same basic wave number as the traveling waves are considered. This constitutes only a part of the whole stability analysis, and subharmonic perturbations (d_m, with $m\neq 0$) also need to be considered in order to complete it.

In Fig. 1 we plot the Reynolds number for which a superharmonic bifurcation appears. All traveling waves belonging to the *upper branch* with Reynolds number from R_N to the values in the curve labeled by $d=0$ are stable to this type of perturbation. In contrast to the case of thermal Rossby waves, a bifurcation with $\Im(\lambda_m)=0$ (mean flow instability) has not been found to be dominant, and then a quasiperiodic time-dependent regime appears. So for any value of α, the bifurcation is a Hopf bifurcation. The corresponding frequencies are plotted in Fig. 2, where we include the fundamental frequency of the traveling waves at the bifurcation point. In this figure we also indicate the parity of the dominant disturbances. Dominant *odd* disturbances would give rise to a bifurcated solution with the same symmetry (3.2) as that of the traveling waves. In Fig. 3 we plot the mean flow of the traveling wave (the parabolic profile is not included) and that corresponding to the dominant disturbance (real and imaginary parts of the y derivative of the zero Fourier mode), at bifurcation points belonging to different zones where a jump of frequencies has appeared.

Superharmonic bifurcations have been obtained by [8] and [3] for $\alpha=1.1$ by using the same method employed here, but with less resolution in the streamwise direction. Our results agree with those obtained by them for a Fourier trun-

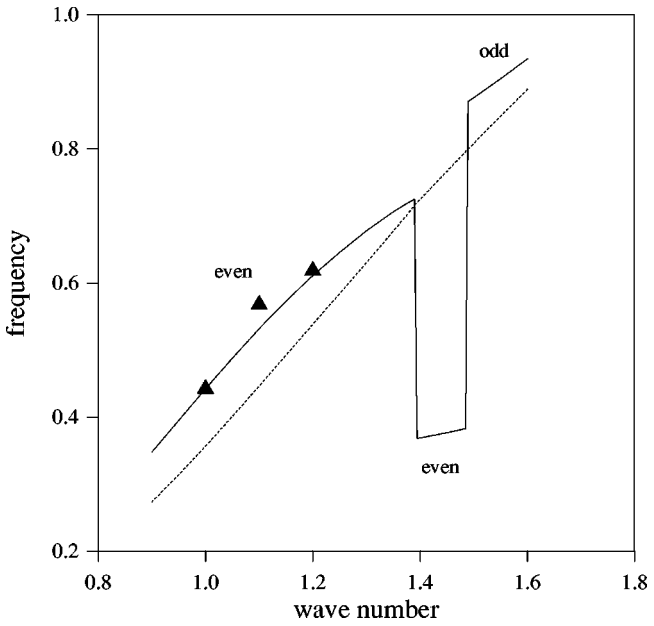

FIG. 2. Frequencies of the Hopf bifurcation corresponding to superharmonic bifurcations (solid line) plotted in Fig. 1 and that corresponding to the traveling waves in the bifurcation point (dotted line) versus the wave number α. We have included results obtained by [2] (solid triangles) by using a time-dependent code. Labels *even* and *odd* mean the type of disturbances that are responsible for the bifurcation; see text.

cation $N=1$ and $N=2$. However, for $N=3$ and $N=4$, we obtain a different period than that plotted in Table 2 in [3]. We believe there may be a misprint in that table, since the period for $N=3$ does not agree with the imaginary part of the eigenvalue (frequency of the Hopf bifurcation) plotted in Fig. 2 of the same paper. We have calculated the period associated with this frequency and have obtained the same result.

Although for analyzing superharmonic stability [1] indicates that the results become roughly stabilized for more than $N=7$ and $J=33$, we present in Table I the results for different truncations to show how the results fluctuate. The critical values are obtained by imposing that $|\Re(\lambda)|<10^{-7}$. The values plotted in Figs. 1 and 2 have been obtained by using a truncation $N=14$ and $J=60$, which guarantees an error of less than 1% in the values of the Reynolds number and in the period for the Hopf bifurcation.

Bifurcated solutions from superharmonic bifurcations have been analyzed by [1] and [2] (short boxes) by using a time-dependent code, for values of $\alpha\approx 1$. Since the bifurcation seems to be supercritical, from this author's results one can deduce the Reynolds number for which this bifurcation sets in. Furthermore, the period of the zero Fourier mode gives information about the frequency of the Hopf bifurcation. We have compared our results with those of this author and, as can be seen in Fig. 2, they agree quite well.

B. Subharmonic bifurcations

In this section we present the results corresponding to subharmonic bifurcations ($d\neq 0$). We suppose that the periodic box contains M structures of periodicity $a=2\pi/\alpha$ and we have analyzed their stability from any perturbation

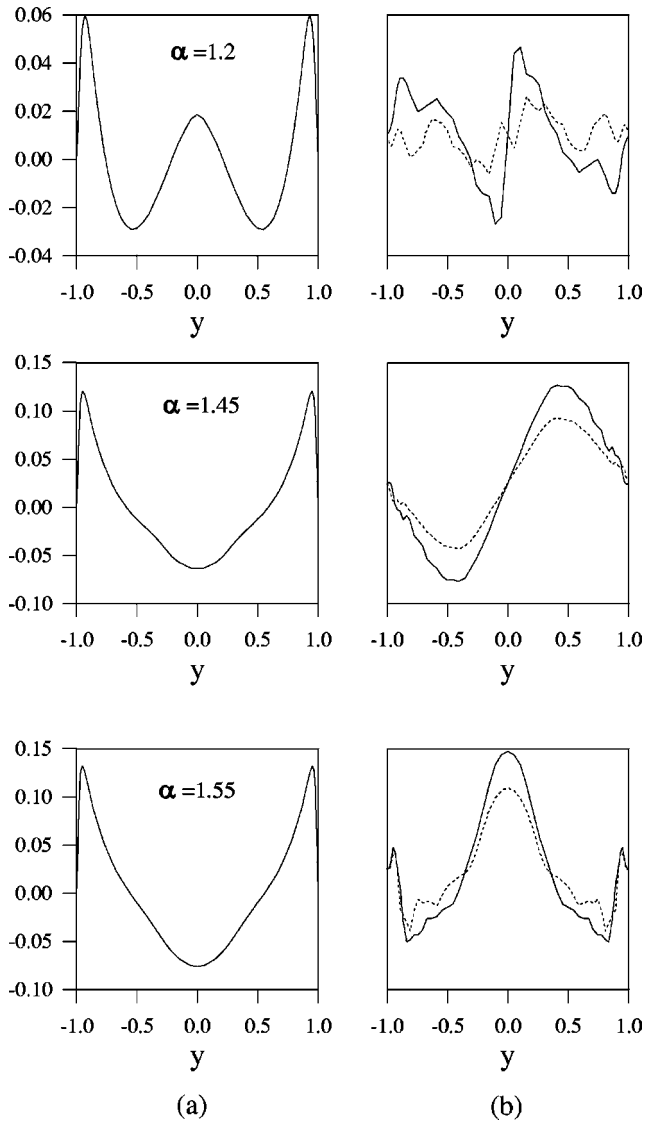

FIG. 3. (a) Mean flow of the traveling wave (the parabolic profile is not included) and (b) real (solid line) and imaginary (dotted line) part of the mean flow corresponding to the most unstable disturbance for different points in the marginal curve corresponding to superharmonic bifurcations. The values of α at these points are 1.2, 1.45, and 1.55.

which, maintaining the periodicity Ma, breaks the basic periodicity a. Hereafter we will denote by α' the wave number associated with the periodic channel, so $\alpha'=\alpha/M$. In this case, disturbances of the form (2.10) also separate into *even* and *odd* disturbances. However, the bifurcated solution would manifest a symmetry only in the case where the *equivalent* subharmonic linear stability analysis was for an odd value of M^* and *even* disturbances for m^* odd (vanishing b_{nj} for $n+j$ odd) or *odd* disturbances for m^* even (vanishing b_{nj} for $n+j$ even). Then, the bifurcated solution, characterized by a symmetric mean flow, would have the following symmetry:

$$\Psi(x,y,t)=-\Psi\left(x+\frac{M^*a}{2},-y,t\right). \tag{3.3}$$

Here, we have analyzed mainly the cases $M=4$ and $M=8$.

TABLE I. Tabulation of the Reynolds number and period T at the superharmonic bifurcation for $\alpha=1.1$ for different values of N and J.

N	J	Reynolds	T
4	40	5803.2	11.60
4	70	5812.6	11.62
8	40	5091.0	11.82
8	50	5056.0	11.84
8	60	5054.0	11.84
12	40	5778.9	11.24
12	50	5189.0	11.80
12	60	5189.1	11.82
14	40	5840.3	11.38
14	50	5386.1	11.62
14	60	5221.2	11.80
16	40	5970.8	11.29
16	50	5424.9	11.62

As we discussed in Sec. II, we have considered disturbances of the form (2.10) for values $d_m=1/M, \ldots, \frac{1}{2}$.

In Fig. 4 we have plotted with dotted lines the values of the Reynolds number as a function of the basic wave number α that limit the zone where a periodic traveling wave of periodicity a contained in a box of periodicity $4a$ is linearly stable to this type of perturbation. For this analysis, it is necessary to consider two values of d_m, $d_1=\frac{1}{4}$ and $d_2=\frac{2}{4}$. As can be seen in the figure, the stability limits of a configuration of four Tollmien-Schlichting waves are due to subharmonic perturbations, except in a region near $\alpha=1.4$. Since the subharmonic stability zone is always associated with the

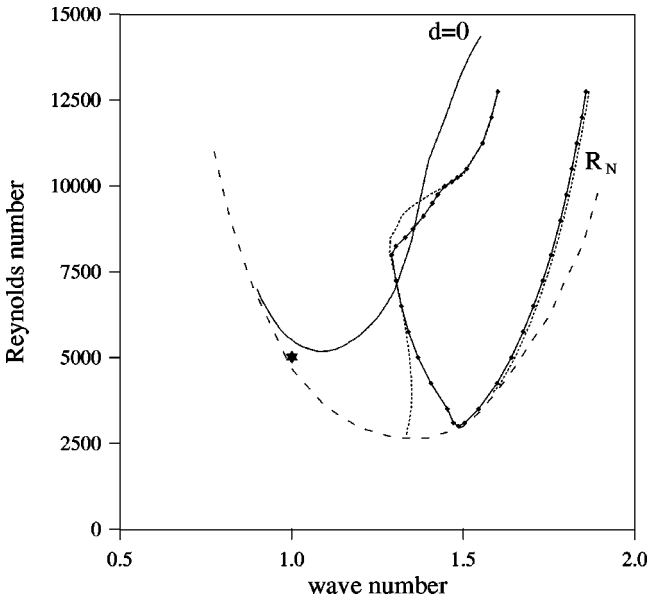

FIG. 4. Reynolds number versus basic wave number corresponding to subharmonic bifurcation points of periodic traveling waves in a box that contains $M=4$ basic wavelengths (dotted line) and $M=8$ wavelengths (dotted-solid line). The curve labeled $d=0$ corresponds to subharmonic bifurcation, and the curve labeled R_N corresponds to *nose* points. We have denoted by an asterisk a point where [2] obtained a stable train of wave packets.

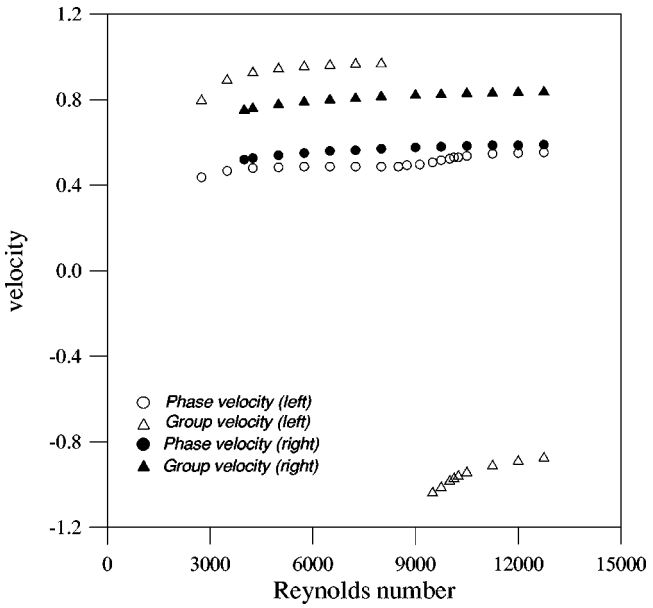

FIG. 5. Phase speed and estimated group velocity versus Reynolds number at the subharmonic bifurcation points displayed in Fig. 4 for a box that contains $M=4$ wavelengths. For a given Reynolds number, circles and triangles correspond to the phase speed and estimated group velocity at the bifurcation points for lower wave number (left side), and solid circles and solid triangles to those for higher wave number (right side).

value d_1, wherever this instability dominates a new solution with periodicity $4a$ emerges. As we explained in a previous section, as a result of this bifurcation, which is always oscillatory, new subharmonic wave numbers and frequencies appear and we can estimate a group velocity by the expression (2.11). In Fig. 5 we have plotted for different values of the Reynolds number the estimated group velocity and phase velocity of the traveling waves at the two points (left and right) which limit the stability zone. Circles (left) and solid circles (right) denote the phase velocity and triangles (left) and solid triangles (right) denote the estimated group velocity.

In Fig. 4 we denote by an asterisk one point (Re$\approx$5000, $\alpha=1$) in which [2] obtained a stable train of wave packets. This author used a time-dependent code and, starting from a established nonlinear wave train of $\alpha=1$, the solution was extended periodically and perturbed slightly. The box is long enough to contain at least four wavelengths ($\alpha'=0.25$). Notice that this point remains outside of the zone where $M=4$ wave trains are stable, which confirms our findings. In addition, Jimenez says that the phase speed of the individual waves ($c\approx 0.35$) is similar to that of the uniform wave trains, but the propagation speed of the groups is faster ($c_g \approx 0.75-0.8$). Similar results were obtained by [7] for the case $M=10$, $\alpha=1$, and Re$=2400$, and the wave packets propagated at a constant velocity $c_g\approx 0.7$, while the constituent waves progressed with about half the wave packet velocity.

If we look for the estimated value of the group velocity (5) at Reynolds number Re$=5000$, on the left side of the curve that limits the stability zone ($\alpha_c=1.35$), we obtain $c_g\approx 0.95$ and a phase speed $c_{TW}=0.48$, which are close to Jimenez's results. We can appreciate the effect of this insta-

bility if we approximate the bifurcating solution at this point by a superposition of the basic wave train and the linear eigenmode. In Fig. 6(a) we display a shaded plot of the vorticity $\omega=-\Delta\Psi$ at $y=-1$ as a function of $x\in(0,2\pi/\alpha_c')$ at a time sequence from $t=0$ to $t=2(2\pi/\omega_{TW}')$, where ω_{TW}' is the fundamental frequency of the uniform wave train ($M=4$) at the bifurcation point Re$=5000$, $\alpha_c=1.35$. Notice how the propagation of the groups is approximately twice the phase speed of the individual waves. In the following section we will show how this type of plot reproduces the behavior of the solution near the bifurcation point. To appreciate the effect of a negative group velocity (the groups travel in the opposite direction to the individual waves) we also display in Fig. 6(b) a similar plot for the bifurcation point Re $=9500$, $\alpha_c=1.36$, and $\alpha_c'=0.34$. The estimated group velocity and phase speed of the traveling wave are $c_g\approx -1.03$, and $c_{TW}=0.51$, respectively.

We have also checked if for a channel of periodicity $\alpha'=0.25$ and for some of the Reynolds numbers analyzed by [2], stable uniform wave trains could appear. The results from our subharmonic stability analysis show that at least for Re$=4000$ and Re$=5000$, a structure containing $M=6$ Tollmien-Schlichting waves ($\alpha=1.5$) would remain linearly stable.

In Fig. 4 we also plot with a dotted-solid line the values of the Reynolds number that limit the stability zone for a periodic box containing $M=8$ uniform wave trains, also considered by [2], and in Fig. 7 (similar to Fig. 5) the corresponding phase velocity and estimate group velocity at the bifurcation points. The marginal curve (α, Re) for the case $M=8$ is close to the marginal curve for the case $M=4$, except in the zone where the superharmonic instability dominates, and also in the neighborhood of the minimum of the *nose* curve, where the $M=8$ curve narrows notably. In addition, notice that for $M=8$ there is a small gap between the *nose* curve and the marginal curve for the subharmonic instability. On the left side of the marginal curve, for Reynolds numbers Re$>10\,000$, the marginal curve coincides with the curve for $M=4$. This is because the dominant subharmonic instability is for $d_2=\frac{2}{8}$, which is the same analysis as $d_1=\frac{1}{4}$ for the $M=4$ case. Save for this zone, the dominant subharmonic analysis is for $d_1=\frac{1}{8}$.

There exist other 2D solutions that might come from a subharmonic bifurcation of the traveling waves. These are the solutions quoted in the previous section, obtained by [13] for $\alpha'\approx 0.3$. We suppose that they come from a traveling wave in a box that contains $M=3$ basic wavelengths. We base this supposition on the results shown in Table 3 in [13] (Re$_Q=2723$, $\alpha'=0.3387$). Here, the value of the phase velocity corresponding to the odd part of Fourier mode $n=3$ (this is the mode of maxim energy) of the x component of the velocity is the same ($c=0.315$) as the even part of Fourier mode $n=6$. This is the parity of modes $n=3$ and $n=6$ in an expansion of an $M=3$ traveling wave. The value of the phase velocity and that of the frequency $\omega_0=0.26$ of the zero odd Fourier mode (ω_0 should be $M=3$ times ω^* at the bifurcation point) could agree with the results we have obtained from a subharmonic instability for the case $M=3$. We have checked this instability for one of the smaller values of the Reynolds number on the left side of the marginal curve for $M=3$ (not plotted in this paper), and we have obtained, for Re$=2950$, $\alpha_c'=1.24/3=0.41$, $c=0.410966$, and $\omega^*=-0.187$. Although the phase velocity and the associated frequency of the zero Fourier mode at the bifurcation point ($\omega_0\approx 0.56$) are higher, in the next section we will show that these values decrease when α' does.

C. Nonperiodic solutions

In this section we wish to show how a stable wave train of Tollmien-Schlichting waves evolves when the size of the periodic channel varies, allowing a subharmonic instability to act on it. In particular, we have considered a fixed Reynolds number Re$=4250$, and starting from a periodic channel that contains a structure formed by $M=4$ uniform wave trains ($\alpha'=0.35=1.4/4$; see Fig. 4), we have obtained different perturbed solutions; those which when α' reaches a value of 0.25 look similar to the wave packet obtained by [2] for this periodicity. This sequence is displayed in Fig. 8, where the vorticity $\omega(x,-1,t)$ (lower wall) is plotted at a sequence of time from $t=0$ to $t=100$ for different values of α'. Notice that the propagation speed of the groups is faster than the phase speed of the individual waves, in agreement with our results in the previous section: For this value of Reynolds number, the subharmonic instability appears for $\alpha_c=1.35$, the phase speed is 0.48, and the estimated group velocity is 0.93. As the value of α' decreases, so does the group velocity and the phase speed, which would be in agreement with the results obtained by [2] at $\alpha'=0.25$ ($c\approx 0.35$, $c_g\approx 0.75-0.8$). The same occurs with the frequency of the zero Fourier mode: for $\alpha=1.3$: this frequency is $\omega_0\approx 0.58$ ($\omega_0\approx 4\omega^*$, since the dominant subharmonic bifurcation is for $d=\frac{1}{4}$), and for $\alpha=1$, this value is $\omega_0=0.38$. This behavior could explain the difference between the results obtained by [13] and our subharmonic instability results, quoted in the previous section for the case $M=3$.

Another aspect worthy of note is the coexistence of solutions for a given periodicity. These solutions come from perturbations of different number M of wave trains. For example, for Re$=4250$, in a periodic channel of $\alpha'=0.25$ one could find the solution that comes from $M=4$ wave trains of periodicity $\alpha=1$ [wave packet in Fig. 8(d)], which is far from its bifurcation point; the solution displayed in Fig. 9(a) that comes from $M=5$ wave trains of periodicity $\alpha=1.25$, which is near to its bifurcation point ($\alpha=1.38$), and the stable $M=6$ wave trains of periodicity $\alpha=1.5$ [see Fig.9(b)].

We have also analyzed how these different configurations are interconnected. To make the discussion more understandable, we have used the length of the periodic box, L, as a parameter, and we have drawn a diagram in Fig. 10 that outlines the connection: where solid lines represent stable M uniform wave trains and dashed lines represent nonperiodic solutions that bifurcate from them. The subharmonic stability analysis tells us that, for Re$=4250$, $M=4$ uniform wave trains are stable in periodic boxes of lengths between $L_{4,min}=15.6$ and $L_{4,max}=18.6$, $M=5$ in boxes between $L_{5,min}=19.6$ and $L_{5,max}=22.7$, and $M=6$ in boxes between $L_{5,min}=23.5$ and $L_{5,max}=27.0$. Thus, when starting from a stable $M=4$ uniform wave train, we increase continuously the length of the box, and we obtain at $L=25.13$ the solution displayed in Fig. 8(d). If we go on increasing L, the $n=4$

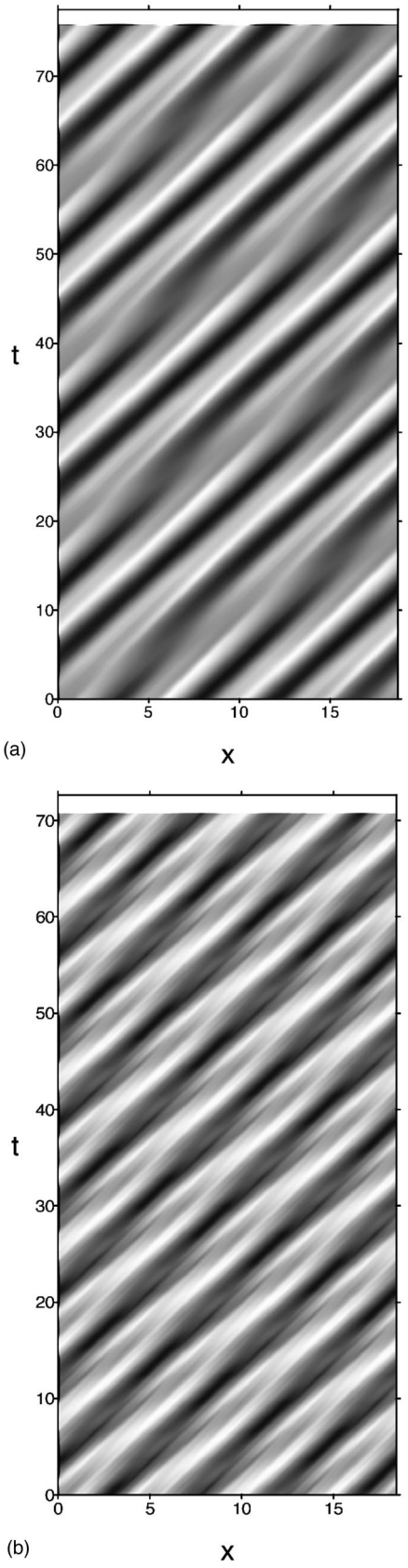

FIG. 6. Shaded space-time plot of the vorticity $\omega(x,-1,t)$ of an approximated bifurcated solution (see text) as a function of $x \in (0,2\pi/\alpha_c')$ at a time sequence from $t=0$ to $t=2(2\pi/\omega_{TW}')$. The values of ω_{TW}' and α_c' are the fundamental frequency and wave number of the $M=4$ traveling waves at the bifurcation point: (a) Re=5000 (left), (b) Re=9500 (left).

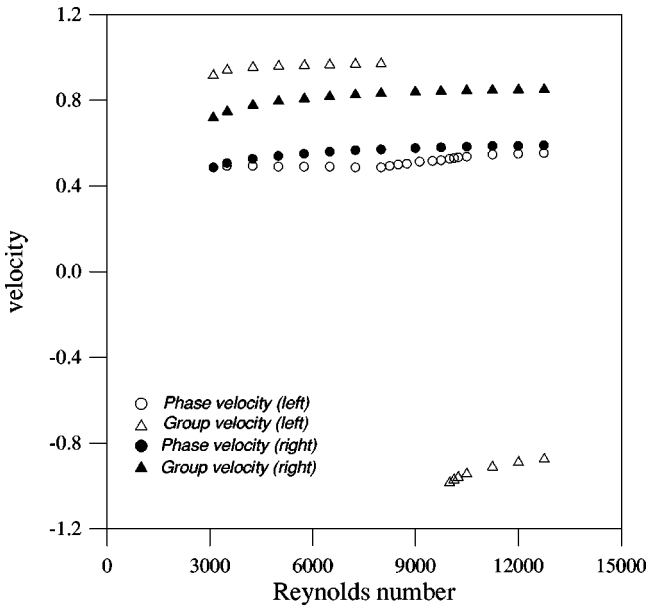

FIG. 7. As in Fig. 5 for $M=8$.

Fourier mode of this solution decreases, while the $n=5$ increases, until at a certain value $L_{4,5}$, this solution coincides with that coming from a subharmonic bifurcation of an $M=5$ uniform wave train. Then, if we decrease the value of L, at $L=25.13$ we obtain the solution displayed in Fig. 9(a), which for $L=L_{5,\max}$ becomes an $M=5$ uniform wave train. If starting again from the solution obtained at $L_{4,5}$ we increase L, we obtain at some value $L_{5,6}$ a solution that coincides with that coming from a subharmonic instability of $M=6$ uniform wave trains. Then, if we decrease L once more until $L=25.13$, we obtain the solution plotted in Fig. 9(b). Different behavior is obtained when, starting from a stable M uniform wave train solution, the length of the box is decreased slightly, allowing the subharmonic instability to act on it. In this case, although the subharmonic instability looks as though it is going to act, after a transient, the solution jumps to the solution that comes from the subharmonic instability of $M-1$ uniform wave trains when L increases, which is a sign of a subcritical bifurcation. To show this latter effect, we plot in Fig. 11 the time series of modes $n=4$ and $n=5$ for a value of $L=19.4$, when we use as initial condition the stable $M=5$ uniform wave train solution obtained for $L=19.63$.

IV. CONCLUSIONS

In this paper we have analyzed the competition between superharmonic and subharmonic instabilities of 2D shear traveling waves, contained in a periodic box of a given periodicity, in the problem of 2D Poiseuille flow. We have considered boxes long enough to contain $M=1$, $M=4$, and $M=8$ basic wavelengths $a=2\pi/\alpha$ for any value of α. The case $M=1$ in a periodic box of length $L=a$ can also be understood as the stability analysis, in a periodic box that contains any value M' of basic of wavelengths a ($L'=M'a$), with respect to perturbations that maintain the basic periodicity a (superharmonic stability analysis), This case has been considered by other authors [15,8,3], for some values of α. We have extended their results to any value of α, as

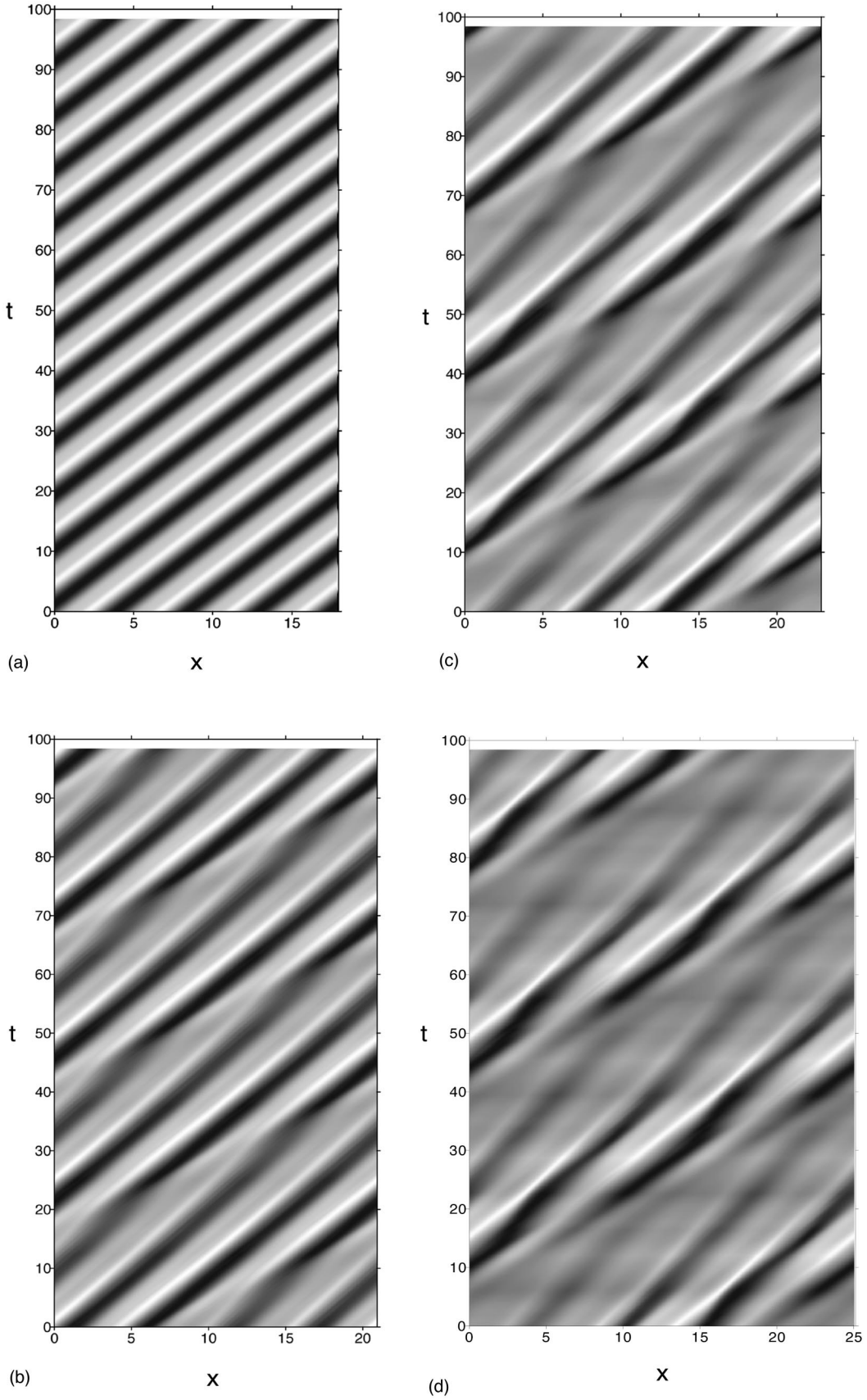

FIG. 8. Shaded space-time plot of vorticity $\omega(x,-1,t)$ (lower wall) as a function of $x \in (0,2\pi/\alpha')$ at a time sequence from $t=0$ to $t=100$ for different values of α'. (a) $\alpha'=0.35$, (b) $\alpha'=0.3$, (c) $\alpha'=0.275$, and (d) $\alpha'=0.25$. The Reynolds number is Re=4250.

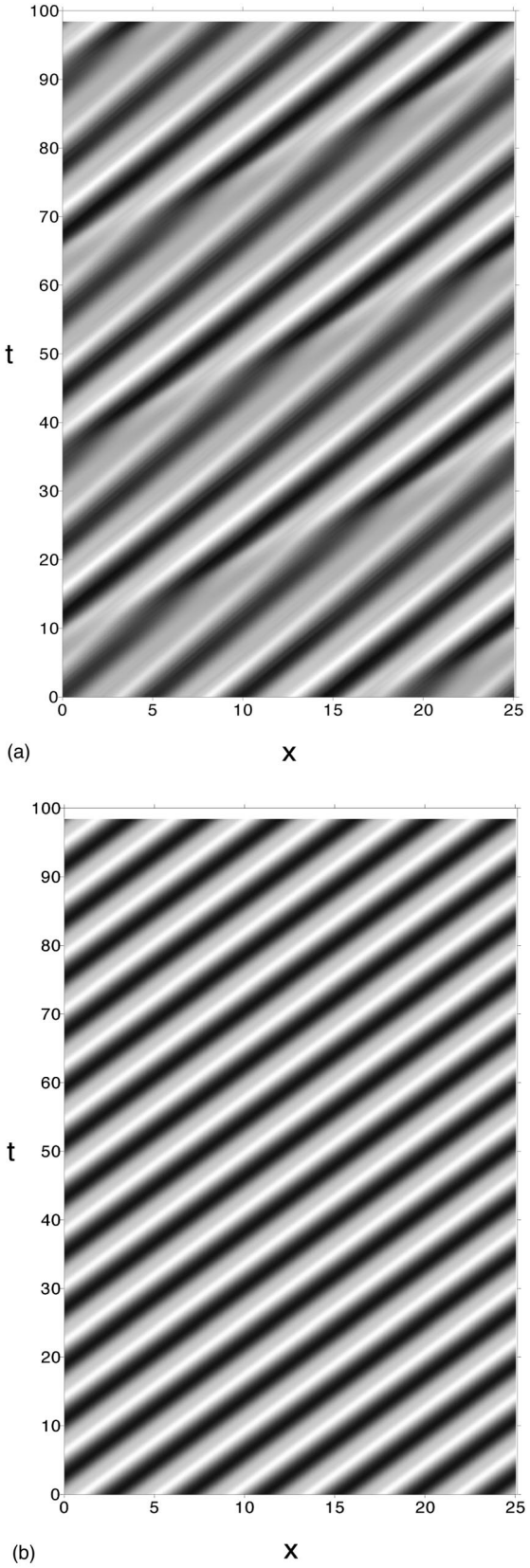

FIG. 9. Shaded space-time plot of vorticity $\omega(x,-1,t)$ (lower wall) as a function of $x \in (0,2\pi/\alpha')$ at a time sequence from $t=0$ to $t=100$ for different configurations obtained with $\alpha'=0.25$. (a) This configuration comes from a subharmonic instability of $M=5$ Tollmien-Schlichting waves ($\alpha=1.25$), and (b) stable $M=6$ uniform wave train ($\alpha=1.5$). The Reynolds number is Re=4250.

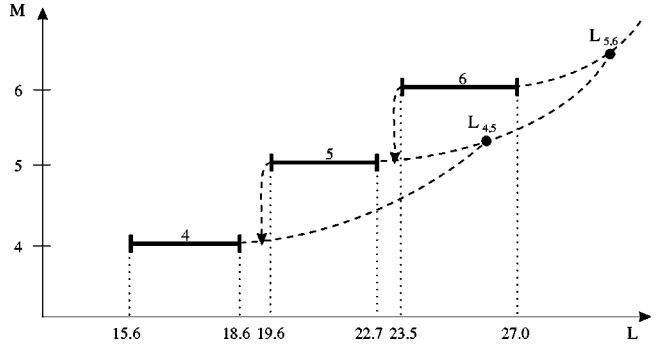

FIG. 10. Diagram that outlines different M solutions obtained in the time dependent simulations as a function of the length of the periodic box L. The Reynolds number is Re=4250.

well as analyzing the symmetry breaking that this bifurcation could give rise to.

The main objective of this paper was to analyze the sequence of bifurcations that, from the basic state, led to stable wave packets, obtained in long boxes by [2] and [7], which extended to very low Reynolds numbers. The manner in which they were obtained in some cases, starting from a

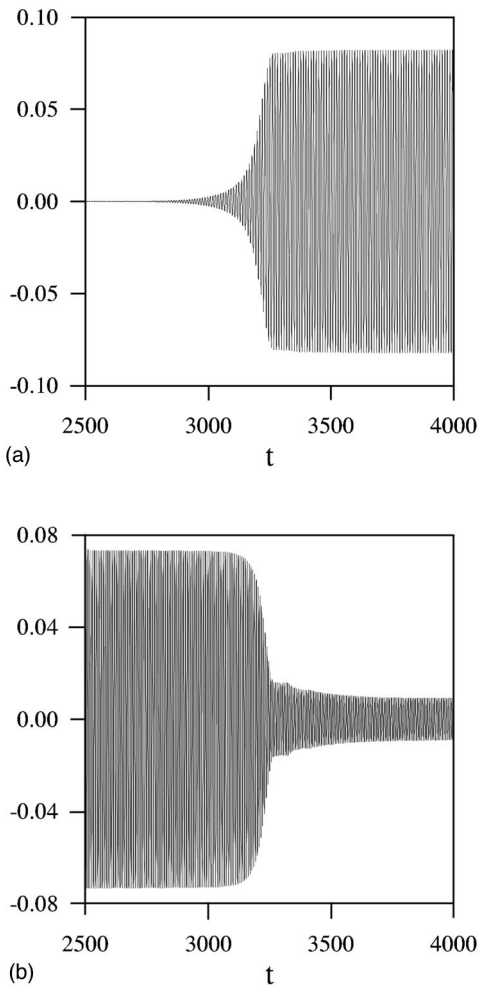

FIG. 11. Time evolution of two different n Fourier modes (a) $n=4$ and (b) $n=5$ in a periodic box of $L=19.4$, starting from the $M=5$ uniform wave train obtained for $L=19.63$. The Reynolds number is Re=4250.

nonlinear wave train extended periodically and perturbed slightly, suggested that they might arise from a subharmonic bifurcation of the periodic wave train. Since this type of bifurcation is oscillatory, it has the minimum ingredients to lead to a wave packet. By employing a method widely used in thermal convection [12] to analyze this type of bifurcation, our results show the existence of a stable zone for the uniform wave trains, outside of which the wave packets were found. For small Reynolds numbers, the estimated group velocity for both cases $M=4$ and $M=8$ is near to the value obtained in the referred works. Although the values of the basic wave number α used by these authors are far from the value on the curve that limits the stability zone, by using a time-dependent code we have shown, that starting from the bifurcated solution and *decreasing* the wave number, the solution evolves continuously to the wave packets. This subharmonic bifurcation behaves in the Poiseuille problem differently from the way it does if the Hopf bifurcation of the basic state is supercritical. In this case, the subharmonic bifurcation can be explained by considering the interaction between different processing modes [17]. If when fixing the control parameter one moves the wave number α, the subharmonic instability, which limits the range of realizable wave numbers, usually has the tendency to shift the basic wave number α of the unstable solution towards the critical wave number. Thus, according to [2,7,10], and [11], the transition of the uniform wave trains towards the localized solutions, when these trains undergo a subharmonic bifurcation by decreasing the wave number, takes place because of the vecinity of the subcritical Hopf bifurcation.

Another question we wished to answer was if stable configurations of uniform wave trains could exist for big boxes. In the results of [2] and [7], these authors used a Fourier spectral decomposition in the x direction, and they stated that they consider four, eight, and ten Tollmien-Schlichting wavelengths in boxes of length $L=8\pi$, 16π, and 20π, respectively. This means that they were working with subharmonic wave numbers of $\alpha=1$, which is clearly outside of the linearly stable zone. This imposition has been critical for obtaining the wave packets. Our results show that, for moderate Reynolds numbers, stable Tollmien-Schlichting waves could be found, provided that their basic wave number was $\alpha\approx 1.5$. This means that the number M of stable uniform wave trains must be related to the length L of the periodic channel by the expression $L\approx M\,2\pi/1.5$. However, other configurations, depending strongly on the initial conditions, can appear in the same channel. These other configurations can be obtained from subharmonic instabilities of uniform wave trains contained in channels of different periodicity.

ACKNOWLEDGMENT

We would like to thank DGYCIT for supporting this work under Grant No. PB94-1216.

[1] J. Jimenez, Phys. Fluids **30**, 3644 (1987).
[2] J. Jimenez, J. Fluid Mech. **218**, 265 (1990).
[3] I. Soibelman and D. I. Meiron, J. Fluid Mech. **229**, 389 (1991).
[4] W. C. Reynolds and M. C. Poter, J. Fluid Mech. **27**, 465 (1967).
[5] P. G. Saffman, Ann. (N.Y.) Acad. Sci. **404**, 12 (1983).
[6] S. E. Orszag and A. T. Patera, J. Fluid Mech. **128**, 347 (1983).
[7] T. Price, M. Brachet, and Y. Pomeau, Phys. Fluids A **5**, 762 (1993).
[8] J. D. Pugh and P. G. Saffman, J. Fluid Mech. **194**, 295 (1988).
[9] U. Ehrenstein and W. Koch, J. Fluid Mech. **228**, 111 (1991).
[10] B. A. Malomed, Physica D **29**, 155 (1987).
[11] O. Thual and S. Fauve, J. Phys. (Paris) **49**, 1829 (1988).
[12] J. Pratt, I. Mercader, and E. Knobloch, Phys. Rev. E **58**, 3145 (1998).
[13] B. L. Rozhdestvensky and I. N. Simakin, J. Fluid Mech. **147**, 261 (1984).
[14] J. P. Zahn, J. Toomre, E. A. Spiegel, and D. O. Gough, J. Fluid Mech. **64**, 319 (1974).
[15] T. Herbert, in *Proceedings of the 5th International Conference on Numerical Methods in Fluid Dynamics*, edited by A. I. Van de Vooren and J. Zandbergen (Springer, New York, 1976), p. 235.
[16] M. Schnaubelt and F. H. Busse, J. Fluid Mech. **245**, 155 (1992).
[17] E. Knobloch, in *Lectures on Solar and Planetary Dynamos*, edited by M. R. E. Proctor and A. D. Gilbert (Cambridge University Press, Cambridge, England, 1994), p. 331.